Mater. Res. Soc. Symp. Proc. Vol. 995 © 2007 Materials Research Society 0995-G02-03

Electronic Structure of Si/InAs Composite Channels

Marta Prada, Neerav Kharche, and Gerhard Klimeck
School of Electrical and Computer Engineering, Purdue University, 465 Northwestern Avenue, West Lafayette, IN, 47907

ABSTRACT

This paper reports electronic structure calculations on composite channels, consisting of indium arsenide grown on the technologically relevant (001), (011) and (112)-orientated silicon surfaces. The calculations are performed with NEMO 3-D, where atoms are represented explicitly in the $sp^3d^5s^*$ tight-binding model. The Valence Force Field (VFF) method is employed to minimize the strain. NEMO 3-D enables the calculation of localized states in the quantum well and their dispersion in the quantum well plane. From this dispersion, the bandgap, its direct or indirect character, and the associated effective masses of the valence and conduction band can be determined. Such composite bandstructure calculations are demonstrated here for the first time. The numerical results presented here can then be included in empirical device models to estimate device performance.

Pure InAs QW appears to be a direct bandgap material, with a relatively small gap and effective masses of about one order of magnitude smaller than for pure Si QW of equivalent thickness. Si, on the other hand, has a larger bandgap and has superior thermal and mechanical properties. Thus heteroepitaxy of both components is expected to yield a highly optimized overall system.

For samples grown along the (001) direction, Si is a direct bandgap material, and deposition of an InAs 3nm layer reduces substantially the hole effective mass and slightly the electronic mass, decreasing the magnitude of the gap. Along the (011) and (112)-growth direction, Si QWs are indirect bandgap material, and deposition of a few InAs layers suffies to make the new material a direct-bandgap heterostructure, decreasing significantly the electronic effective mass.

INTRODUCTION

As reduction of feature sizes for semiconductor devices continues in order to achieve higher integration densities, higher speed, lower power consumption and lower costs, channel thicknesses of only a few nanometers are necessary to accomplish near future industry demands. New ultra-thin body (UTB) geometries must be explored to ensure electrostatic control, for which the atomistic texture makes the use of effective mass approach questionable, and an atomistic treatment of the device becomes essential.

Here we apply the semi-empirical tight-binding theory to semiconductor thin films grown on the three most relevant orientations. Atoms are represented explicitly in the Valence Force Field (VFF) method [1] to minimize the strain and in the sp3d5s* tight-binding model. Band structure effects play a crucial role in nanoscale MOSFETs [2]. NEMO 3-D [3] enables the calculation of localized states in the quantum well and their dispersion in the quantum well plane. From this dispersion, the *bandgap*, its direct or indirect *character*, and the associated *effective masses* of the valence and conduction band can be determined.

Silicon based electronic devices remain the undisputed standard in the industry, demanding constant technological improvement. In particular, it is desirable to enhance carrier mobility and improve its optical properties. Carriers in compound semiconductors have, in general, smaller effective mass than those in silicon, leading to higher mobilities. Thus, there is a potential benefit from the integration of compound semiconductors with the mature technology of silicon.

Sophisticated crystal growth techniques have enabled researchers to rise up to the challenge of integrating III-V semiconductors with silicon [4-8]. Here we focus on the potential of InAs, a compound material characterized by a very low effective mass. Silicon has superior thermal and mechanical properties, whereas InAs is superior in electronic and optical properties. The heteroepitaxial systems proposed here exploits the individual properties of the constituents to yield a highly optimized overall system. The authors believe that InAs circuits fabricated on Si substrates could exhibit higher resistance to thermal burnout and runaway than those fabricated on InAs or GaAs substrates. This work considers a 8nm-thick quantum well composed of $Si_{1-x}InAs_x$ where x is 0,1,2,3,4, and 8nm, grown along the standard (001) direction, and the more technologically relevant (011) and (112) [9].

According to the *model solid theory* [10], a deforming potential causes the bands to shift with respect a reference absolute value. This absolute value is chosen in our calculations to be referred to the valence band of the Si, although any other choice could be valid. Thus, the Si tight-binding parameters have been calibrated in NEMO-3D to match the band-offsets accordingly. Further bending is obtained numerically, as represented in Fig 1, which represents local band structure numerical results for the unit cell represented in the inset: ~2nm of InAs deposited on ~6nm of Si. We observe band bending in accordance to Van der Walle's model solid theory.

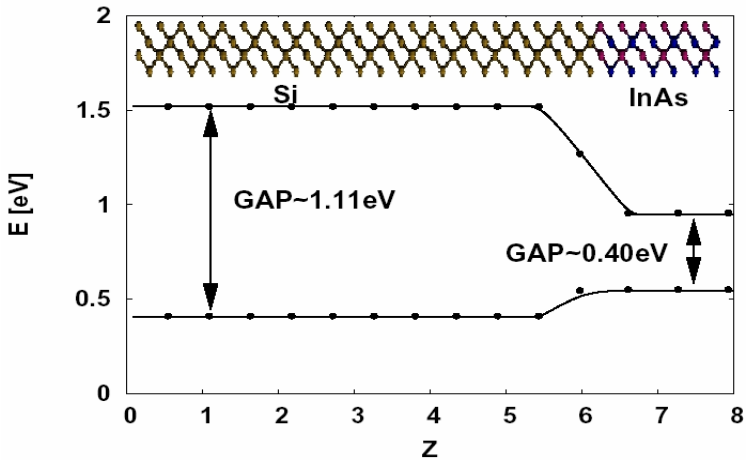

Fig. 1. Schematic representation of band shifts in a Si/InAs heterostructure: NEMO-3D numerical results of local band structure. Inset: unit cell of the structure. Lattice mismatch in the heterostructure causes changes in band alignment.

RESULTS

We consider $Si_{1-x}InAs_x$ heterostructures grown along (001), (011), and (112) axes. The total width of the resulting quantum well is chosen to be 8nm. We study the effects on the

electronic properties of the structures as InAs is added to the top of the structure: x=0,1,2,3,4 and 8. The structure is represented by unit cells that consist of a number of atoms that can constitute the entire QW upon infinite repetition. Thus, the periodicity of the numerical simulations allow performance using only the atoms included in the unit cell (limited to 13 zinc-blende unit cells, or 104 atoms, in most of the cases), resulting in very short computation times.

In all the cases periodicity is biaxially applied for both strain and electronic calculations over the plane perpendicular to the growth direction. Strain causes the lattice constant to change along the growth direction. For convenience, we apply fixed boundary conditions for the lattice constant to the Si value on the bottom of the QW, and allow NEMO-3D to minimize the strain energy by varying the lattice constant along the *z*-axis.

(001)-Orientated Si Surface

The widely used (001) direction for heteroepitaxy growth is considered first in this work. 8nm-silicon quantum wells grown in this fashion show a conduction band minima in Γ, a situation preserved with the deposition of InAs. Fig. 2 shows the progressive improvement of the effective masses as *x* increases, although a substantial decrease in the bandgap is observed.

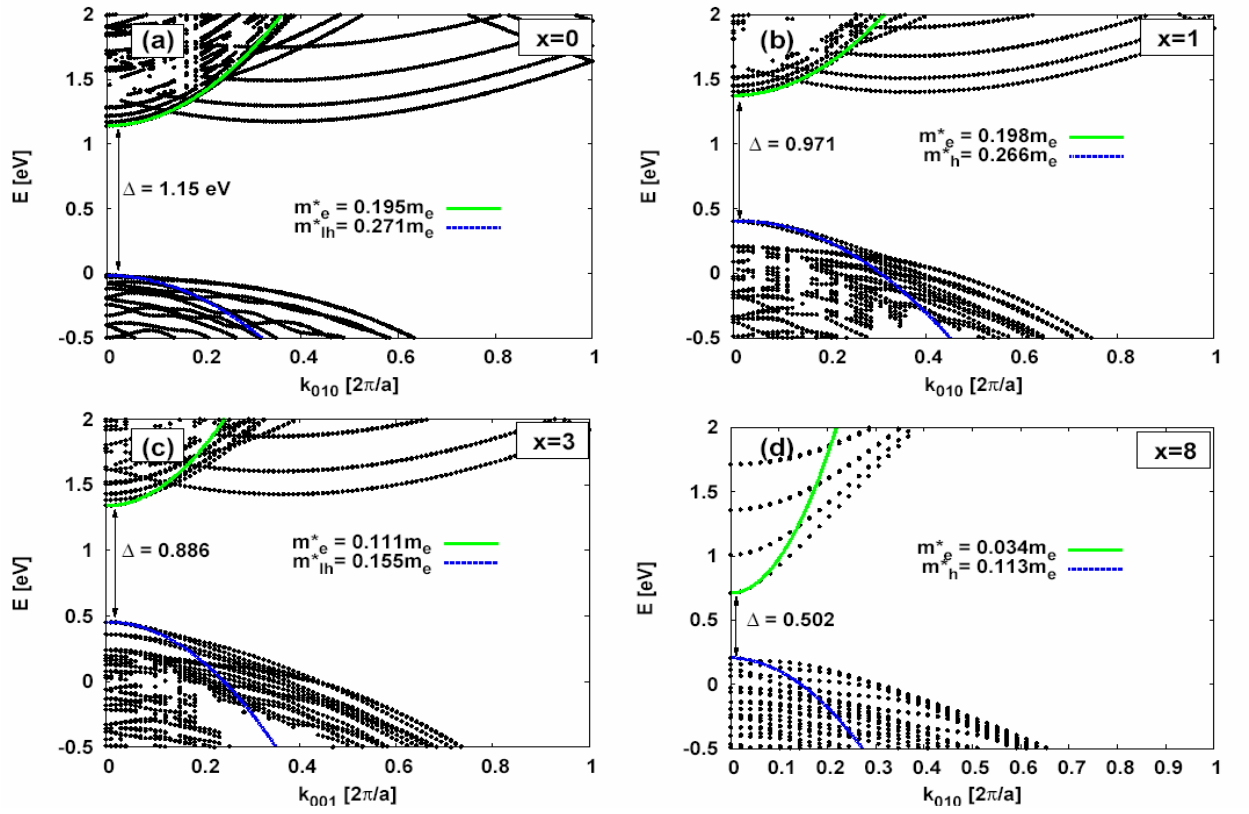

Fig 2. Numerical results obtained with NEMO-3D for the dispersion of a ~8-nm width $Si_{1-x}InAs_x$, heterostructure, x being the thickness (in nm) of the InAs layer: (a) x=0, or pure Si QW, (b) x=1, (c) x=3, (d) x=8 or pure InAs QW.

(011)-Orientated Si Surface

We consider next the technically relevant (011) growth directions, where the surface charge dipoles are balanced. The unit cell is tilted in the *xz* plane for convenience. In contrast to the (001) case, the Si QW appears to be an indirect-gap structure, a situation that changes with the addition of InAs layers, as shown in Fig. 2(b): the gap decreases only slightly, whereas the effective mass decreases substantially as *x* is incremented, representing an optimized compromise. We find the best device characteristics by deposition of x=3nm of InAs, where the effective electronic mass is reduced from $0.927m_e$ to $0.147m_e$, whereas the gap is reduced only by 43meV.

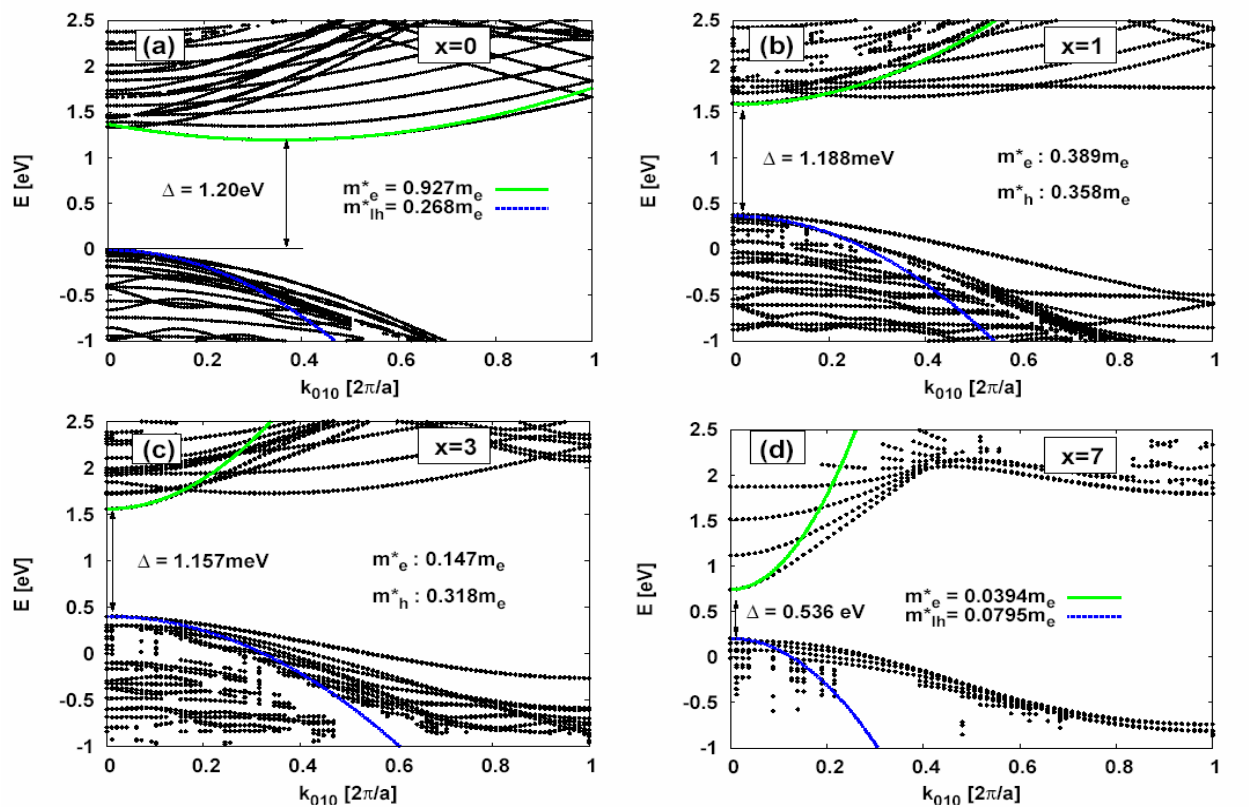

Fig 4. 8-nm width $Si_{1-x}InAs_x$, QW growth along the [110] direction. (a) x=0, or Si QW, (b) x=1, (c) x=3, (d) x=8 or InAs. For x=0, the GAP is indirect, a situation that changes for x>0.

(112)-Orientated Si Surface

For a (112) oriented structure, a Si-8nm QW is indirect band-gap material, a similar situation to the (011) oriented structures. However, deposition of x=1nm InAs layer is not sufficient to make the resulting heterostructure a direct-bandgap material. Direct bandgap character is observed only for $x \geq 3$nm, where we find the effective electronic mass is reduced only by a 20% of its pure Si value, and the gap is reduced by 327meV.

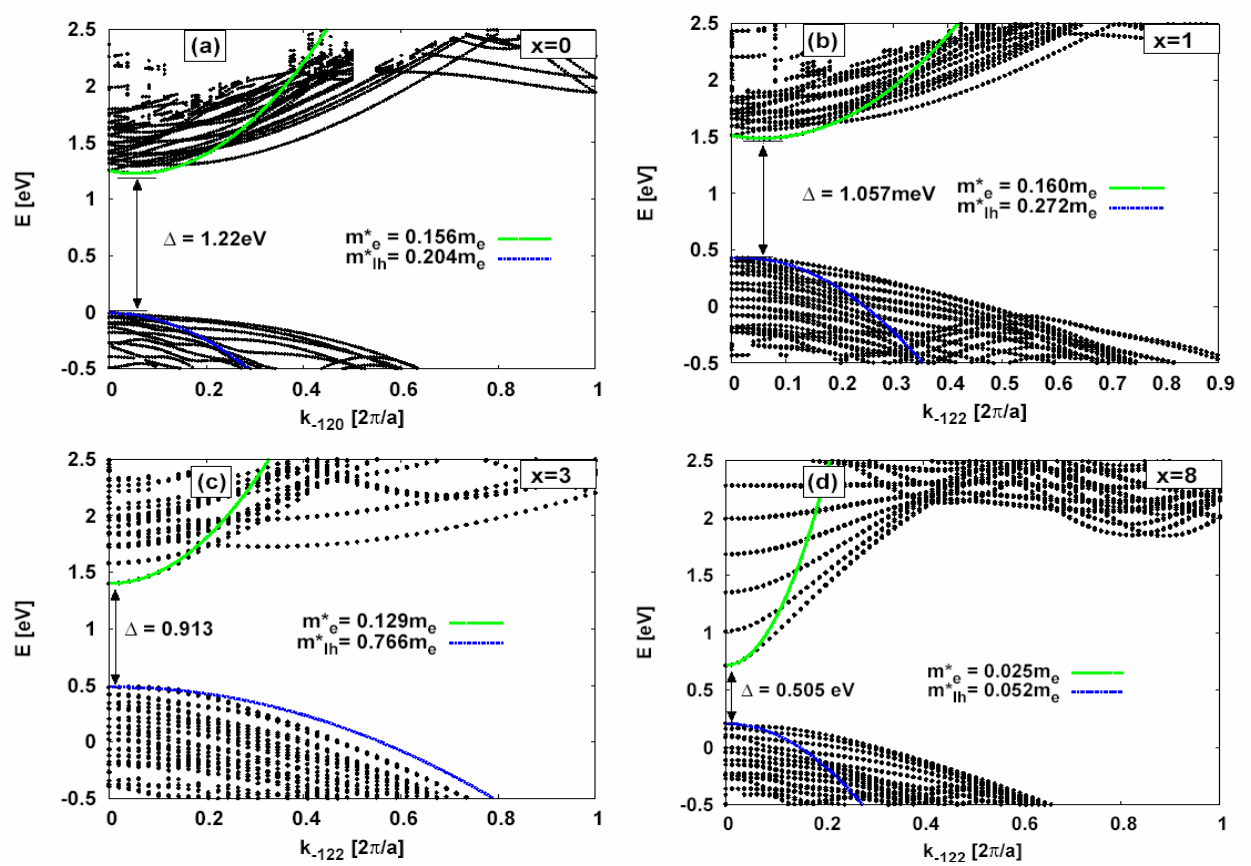

Fig. 4: . 8-nm width $Si_{1-x}InAs_x$, QW growth along the [211] direction. (a) x=0, or Si QW, (b) x=1, (c) x=3, (d) x=8 or InAs. For x=0,1 and 2nm the GAP is indirect, a situation that changes for x>3nm.

The data on the three different lattice orientations in terms of direct/indirect gap, gap energy, electron and hole effective masses are summarized in table 1, also represented in Fig. 5. All the parameters converge to the pure InAs QW value as *x* increases, as expected.

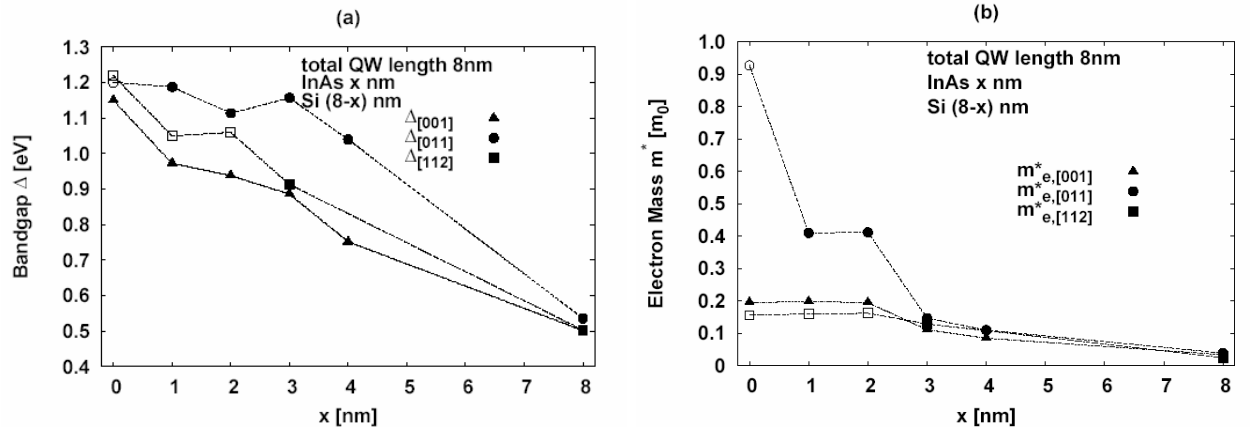

Fig. 5.(a) Bandgap and (b) effective mass for electrons in (001), (011) and (112)-oriented heterostructures as a function of InAs thickness (x). All the values converge to the pure InAs QW. Open symbols correspond to the indirect bandgap situations.

x	0nm (Si QW)			1nm			2nm			3nm			InAs QW		
dir.	(001)	(011)	(112)	(001)	(011)	(112)	(001)	(011)	(112)	(001)	(011)	(112)	(001)	(011)	(112)
$\mathbf{m^*_e}$	.195	.927	.156	.198	.389	.160	.195	.412	.162	.085	.147	.129	.034	.039	.025
$\mathbf{m^*_h}$	.271	.268	.204	.266	.358	.272	.180	.452	.190	.124	.318	.766	.113	.079	.052
gap	1.15 DBG	1.20 **IBG**	1.24 **IBG**	.975 DBG	1.18 DBG	1.06 **IBG**	.938 DBG	1.18 DBG	1.06 **IBG**	.886 DBG	1.16 DBG	.913 DBG	.502 DBG	.536 DBG	.505 DBG

Table 1: Energy gap, electron and hole effective masses, for (001), (011) and (112)-oriented $Si_{1-x}InAs_x$ heterostructures.

CONCLUSIONS

The calculations presented in this work can be included in empirical device models, to estimate their performance. For structures grown along (001), Si has a direct band-gap character, in contrast with (011) and (112) grown. The electronic effective mass decreases with the InAs thickness, but on the other hand, the BG goes smaller as one increases the thickness of the InAs. Therefore, it is crucial to find a heterostructure that optimizes the electronic properties.

We find that of the three studied orientations, the best improvement upon InAs deposition is found for the (011) oriented Si/InAs heterostructure. The (112)-oriented case presents little improvement after addition of InAs. The smallest effective mass is found in the (001) oriented structure, for $x \geq 3$nm.

ACKNOWLEDGMENTS

We acknowledge the valuable discussions with Dr Alan Seabaugh

REFERENCES

1. P N Keating, *Phys. Rev.* **145**, 637–645 (1966).
2. A Rahman, G Klimeck, and M Lundstrom, 2005 IEEE IEDM, 2005
3. G Klimeck, et al., Computer Modeling in Engineering and Science **3**, 601 (2002).
4. N. D. Zakharov, P. Werner, U. G¨osele, R. Heitz, D. Bimberg, N. N. Ledentsov, V. M. Ustinov, B. V. Volovik, Zh. I. Alferov, N. K. Polyakov, V. N. Petrov, V. A. Egorov, and G. E. Cirlin*, Appl. Phys. Lett.* **76** 2677 (2000)
5. G. E. Cirlin, N. K. Polyakov, V. N. Petrov, V. A. Egorov, D. V. Denisov, B. V. Volovik, V. M. Ustinov, Zh.I. Alferov, N. N. Ledentsov, R. Heitz, D. Bimberg, N.D. Zakharov, P. Werner, and U. Goesele, *Material Science and Engineering* **B80**, 108 (2001)
6. S. F. Fang, K. Adomi, S. Iyer, H. Morkoc, H. Zabel, C. Choi, and N. Otsuka, *J. Appl. Phys.* **68** R31 (1990)
7. S. Kalem, J. Chyi, C. W. Litton, H. Morkoc, S. C. Kan, and A. Yariv, *Appl. Phys. Lett.* **53** 562 (1988)
8. T. E. Haynes, R. A. Zuhr, S. J. Pennycook and B. R. Appleton, *Appl. Phys. Lett.* **53** 1439 (1989)
9. private communication, Dr. Alan Seabaugh, Notre Dame.
10. G Van de Walle, *Phys. Rev. B* **39**, 1871–1883 (1989)